

The Diffuse Radiation Field at High Galactic Latitudes

Jayant Murthy,¹  M. S. Akshaya,²  S. Ravichandran,²  R. C. Henry,³  and James Overduin⁴

¹Indian Institute of Astrophysics, Bengaluru 560 034

²Christ University, Bengaluru 560 029

³Henry A. Rowland Department of Physics and Astronomy, The Johns Hopkins University, Baltimore, MD 21218

⁴Department of Physics, Astronomy and Geosciences, Towson University, Towson, MD 21252, USA

Accepted XXX. Received YYY; in original form ZZZ

ABSTRACT

We have used *GALEX* data of the North and South Galactic poles to separate the Galactic and extragalactic components of the diffuse ultraviolet background. We find, consistent with previous observations, an FUV (1531 Å) offset of 261 ± 16 and 263 ± 16 photons $\text{cm}^{-2} \text{s}^{-1} \text{sr}^{-1} \text{Å}^{-1}$ in the NGP and the SGP, respectively. The corresponding offsets for the NUV (2361 Å) are 475 ± 15 and 535 ± 19 photons $\text{cm}^{-2} \text{s}^{-1} \text{sr}^{-1} \text{Å}^{-1}$ in the NGP and the SGP, respectively. Less than 150 photon units are due to extragalactic sources with the remaining 150 (FUV) and 400 (NUV) photons $\text{cm}^{-2} \text{s}^{-1} \text{sr}^{-1} \text{Å}^{-1}$ due to an unidentified source.

Key words: surveys - dust - local interstellar matter - ultraviolet: general - ultraviolet: ISM

1 INTRODUCTION

The diffuse radiation at high latitudes is, by definition, a combination of diffuse Galactic light (DGL) and extragalactic background light (EBL). Much of the DGL is likely to be light from Galactic plane stars scattered by interstellar dust (Jura 1979) and, because there is little dust at the Galactic poles, most of the diffuse light observed in those regions might be expected to be from the EBL (Bowyer 1991; Henry 1991). A listing of all polar observations in the 1200 – 3000 Å spectral range is given in Table 1 with typical fluxes observed to be between 200 – 300 ph $\text{cm}^{-2} \text{s}^{-1} \text{sr}^{-1} \text{Å}^{-1}$ (hereafter photon units).

The largest component of the EBL is the integrated light of galaxies which Xu et al. (2005) found to be 50 and 110 photon units at 1500 and 2300 Å respectively, with similar values of 60 – 76 (FUV) and 121 – 167 (NUV) photon units found by Driver et al. (2016). Somewhat higher values were found in the FUV by Voyer et al. (2011) (55 – 95 photon units) and by Gardner et al. (2000) (144 – 195 photon units). There may be smaller contributions from the integrated light of QSOs (16 – 30 photon units: Madau (1992)) and the IGM (< 20 photon units: Martin et al. (1991)) for a total EBL of < 150 photon units in the UV.

Table 1. Polar Observations

References	Wavelength (Å)	Offset (photon units)
Anderson et al. (1979)	1230 – 1680	285 ± 32
Paresce et al. (1979)	1350 – 1550	300 ± 60
Paresce et al. (1980)	1350 – 1550	<300
Joubert et al. (1983)	1690	300 – 690
	2200	160 – 360
Jakobsen et al. (1984)	1590	<550
	1710	<900
	2135	<1300
Tennyson et al. (1988)	1800 – 1900	300 ± 100
	1900 – 2800	400 ± 200
Onaka & Kodaira (1991)	1500	200 – 300
Feldman et al. (1981)	1200 – 1670	150 ± 50
Hurwitz et al. (1991)	1415 – 1835	300 – 400
Henry & Murthy (1993)	1500	300 ± 100
Murthy & Henry (1995)	1250 – 2000	$100 - 400$
Hamden et al. (2013)	1344 – 1786	300
Murthy (2016)	1531	300
	2361	600

Henry et al. (2015) has argued strongly that there is an additional component to the DGL, unrelated to dust-scattered starlight. Much of the evidence for this component comes from *GALEX* observations of the Galactic poles in the FUV from Murthy et al. (2010). We have used an improved reduction of the diffuse background (Murthy 2014a) with a Monte Carlo model for the dust scattered light (Murthy

* E-mail: jmurthy@yahoo.com

† E-mail: akshaya.subbanna@gmail.com

‡ E-mail: ravichandran.s@christuniversity.in

§ E-mail: henry@jhu.edu

¶ E-Mail: james.overduin@gmail.com

2016) to further explore the background in the vicinity of both Galactic poles in the far-ultraviolet (FUV: 1531 Å) and the near-ultraviolet (NUV: 2361 Å).

2 DATA

The *GALEX* mission (Martin et al. 2005; Morrissey et al. 2007) took observations covering most of the sky in the FUV and NUV bands. Each observation consisted of one or more visits with exposure times of 100 - 1000 seconds which could be summed up to integration times of as high as 100,000 seconds. The original data were distributed as FITS (Flexible Image Transfer System) files with a pixel size of $1.5''$ from which Murthy (2014a) masked out the stars and rebinned to a spatial resolution of $2'$. These data include a foreground from airglow and zodiacal light whose level varies with the observation time and date (Murthy 2014b) which were subtracted from each visit to yield the astrophysical background. The data are available from the High Level Science Products (HLSP) data repository¹ at the Space Telescope Science Institute. Although Murthy (2014a) also produced a map of the diffuse radiation over the entire sky, we have used the visit-level data to study the diffuse radiation at the poles where uncertainties in the foreground subtraction may be important.

We have rebinned the original $2'$ bins of Murthy (2014a) by a factor of 3 (into $6'$ bins) and coadded over all visits in the North Galactic pole (NGP) and the South Galactic pole (SGP). The resultant images are shown in Fig. 1 and Fig. 2, respectively. Although one might expect a good correlation between the FUV and the NUV and between both UV bands and the IR (Hamden et al. 2013; Murthy 2014a), there is much less structure in the NUV image than in the $100\ \mu\text{m}$ images from the *Infrared Astronomical Satellite* (*IRAS*) (bottom panels) or, indeed, in the FUV.

Given that these are archival data, there was no observing strategy in these maps and the number of visits and the exposure times fluctuate wildly. We have plotted the number of visits for the NUV over the NGP in Fig. 3; similar plots could be made for the FUV and the SGP. About 30% of the field around the NGP was covered by single visits with another 25% by two visits. The typical exposure time was about 100 seconds per visit. The remainder included fields with multiple visits with the deepest being the Subaru Deep Field observations with a total exposure time of 164,369 seconds in 169 visits. 12% of the field (black in the figure) could not be observed because of nearby bright stars.

As noted by Murthy (2014b), the foreground emission (airglow and zodiacal light) is dependent on the time and date of the observation but may reasonably be expected to be uniform across the field in a single visit. Murthy (2014b) provided a prescription for the subtraction of the foreground (airglow in the FUV; airglow and zodiacal light in the NUV) but the uncertainty in the foreground subtraction must be considered at high Galactic latitudes where the DGL + EBL is faint.

We have tested our foreground subtraction using the

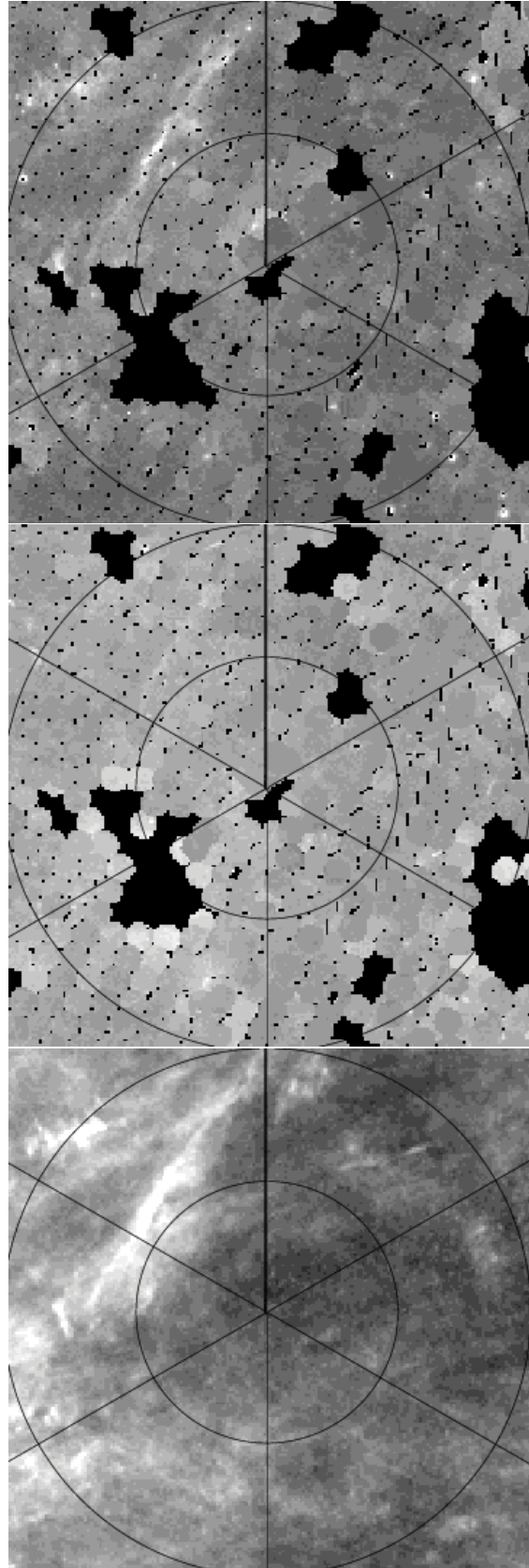


Figure 1. Observed fluxes in FUV (top), NUV (middle) $100\ \mu\text{m}$ flux from the *IRAS* mission (bottom). The scaling is linear from 0 – 800 and 0 – 1200 photon units in the FUV and NUV, respectively, and from 0 – 2 MJy sr^{-1} in the $100\ \mu\text{m}$ map. Black areas were not observed by *GALEX*. The NGP is at the centre with lines of latitude at 80° and 85° and lines of longitude every 60° starting from 0° at the top. MNRAS **000**, 1–9 (2016)

¹ <https://archive.stsci.edu/prepds/uv-bkgd/>

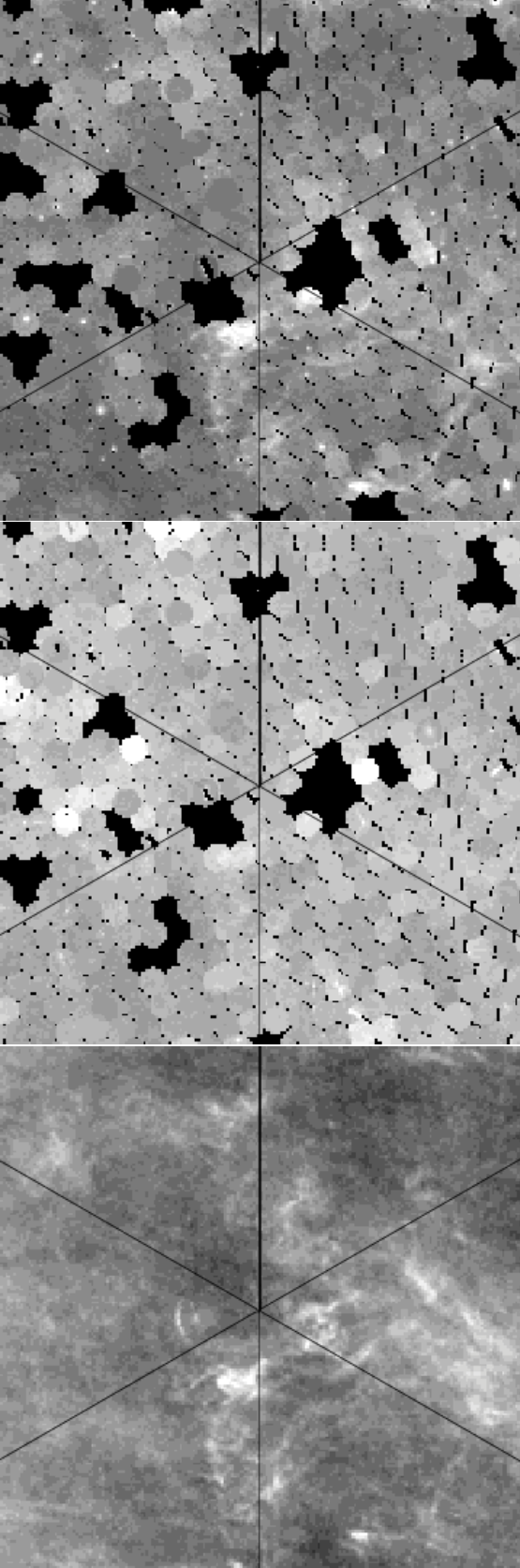


Figure 2. Same as in Fig. 1 but for the SGP.

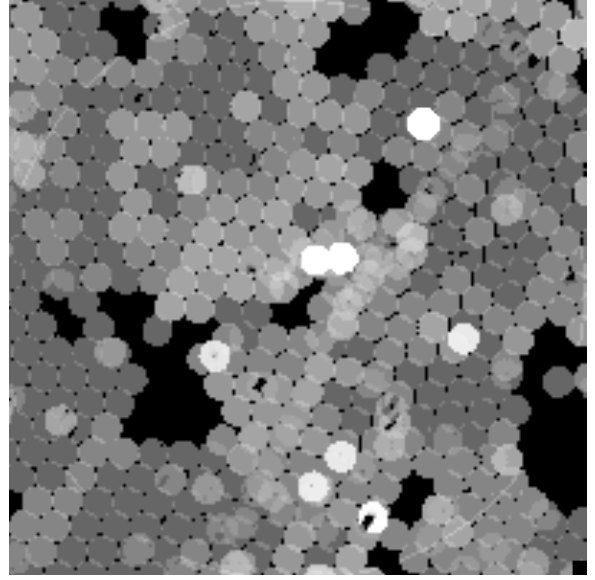


Figure 3. Number of individual visits over the NGP in the NUV band. Black areas were not observed.

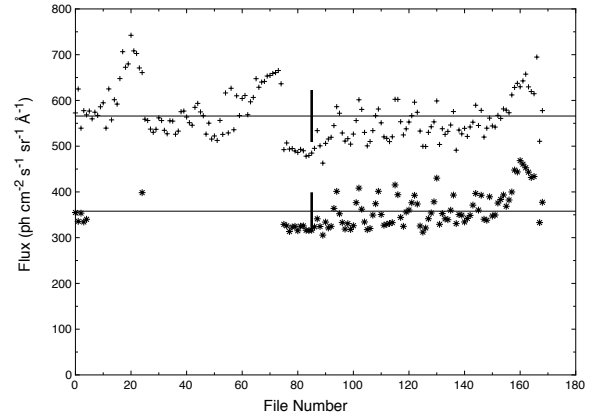


Figure 4. Median values for FUV (*) and NUV (+) in each visit. The horizontal lines show the medians in each band over all visits with the standard deviation plotted as vertical lines in the centre of the plot. Many FUV values are missing because there were no observations on those dates.

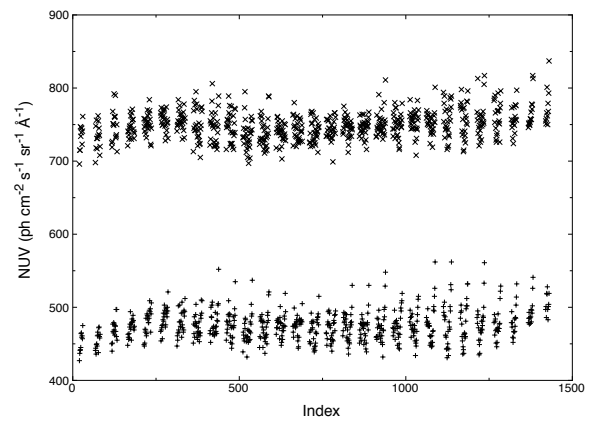


Figure 5. Pixel values for two different visits.

Subaru Deep Field (Kashikawa et al. 2004), which was targeted by *GALEX* (Ly et al. 2009) as part of the overall saturation coverage of that region by a number of different observatories. There were a total of 99 different visits in the FUV and 169 in the NUV with exposure times from 80 – 1700 seconds for each visit and cumulative exposure times over the three years from Apr. 2004 to May 2007 of 83,031 seconds in the FUV and 164,369 seconds in the NUV. Most of the observations were centred at the same point with a few offset by arcminutes. We have chosen a single 6′ bin and tracked its flux over the 169 visits of which 99 included FUV observations (Fig. 4). The mean value is 358 ± 38 photon units in the FUV and 566 ± 54 photon units in the NUV, with the variations in the two bands highly correlated ($r = 0.9$). The difference between two visits is manifested as a uniform increase in the background level of the entire image (Fig. 5). Because the variations in both bands are highly correlated, we believe it is due to an increase in the radiation spacecraft environs.

The astrophysical background (DGL + EBL) will not change between visits and any offset will be due to the foreground, whatever its source. We defined the offset between visits as the difference between the medians, subtracted the offset and coadded them to form the images shown in Figs. 1 and 2. We have adopted the uncertainty found by Murthy (2014a) of 20 photon units in the FUV and 40 photon units in the NUV.

There are a number of bright point-like features in the FUV which are not visible in the NUV, such as the one in the lower right of the NGP image. These are *all* due to instrumental artefacts such as that shown in Fig. 6, in this case around the 9th magnitude star HD 109691. Although, we reject the star in both bands, our automated procedure does not exclude the entirety of the structure around the star in the FUV image leaving an artefact in the FUV maps of Figs. 1 and 2.

The median value of the (foreground-subtracted) FUV background is 339 ± 64 photon units in the NGP and 370 ± 76 photon units in the SGP (Fig. 7) while the median NUV background is 583 ± 66 photon units in the NGP and 652 ± 85 photon units in the SGP. The minimum values for the FUV are 261 ± 16 photon units and 263 ± 16 photon units in the NGP and SGP, respectively, and 475 ± 15 and 535 ± 19 photon units for the NUV in the NGP and SGP, respectively. Taken at face value, these are upper limits for the EBL and match well with earlier determinations of the background (Table 1), including with *GALEX* results from Hamden et al. (2013) and Murthy (2016). As discussed above, the predicted values are <150 photon units for the EBL.

We have plotted the UV fluxes as a function of the 100 μm IR flux in Fig. 8 and have calculated the correlations between the different quantities in Tables 2 and 3. Although the UV and IR background radiation are correlated at lower latitudes (Murthy 2016), we do not find any correlation between the NUV and IR at either pole. The FUV-IR relationship is more complex with no correlation for 100 μm fluxes less than 0.8 MJy sr^{-1} . The brighter IR features, including Markkanen’s Cloud (Markkanen 1979), are clearly seen in the FUV and there is a correlation for larger values of the IR flux. Matsuoka et al. (2011) observed a similar behaviour in *Pioneer* observations of the diffuse optical background and identified the IR offset with the cosmic infrared background

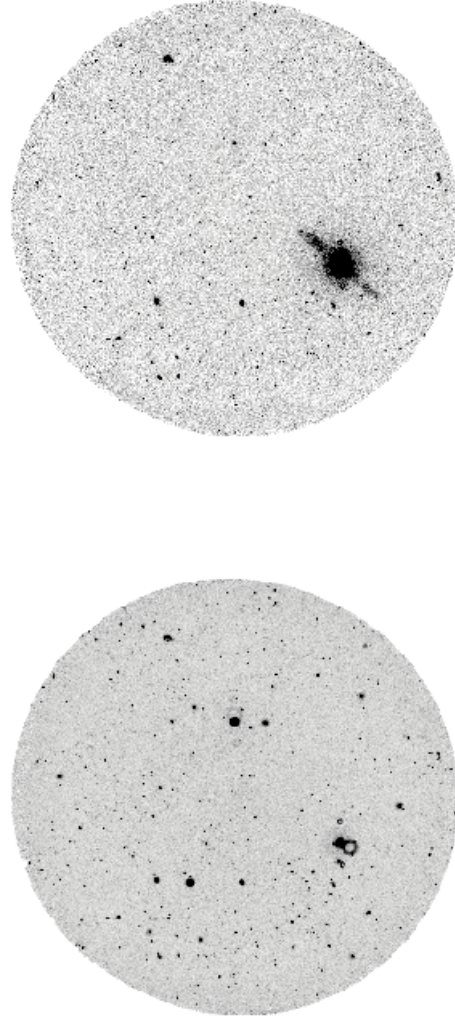


Figure 6. *GALEX* FUV (left) and NUV (right) single visit images.

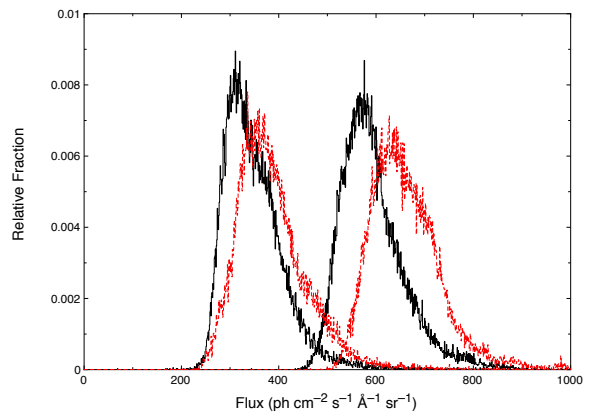


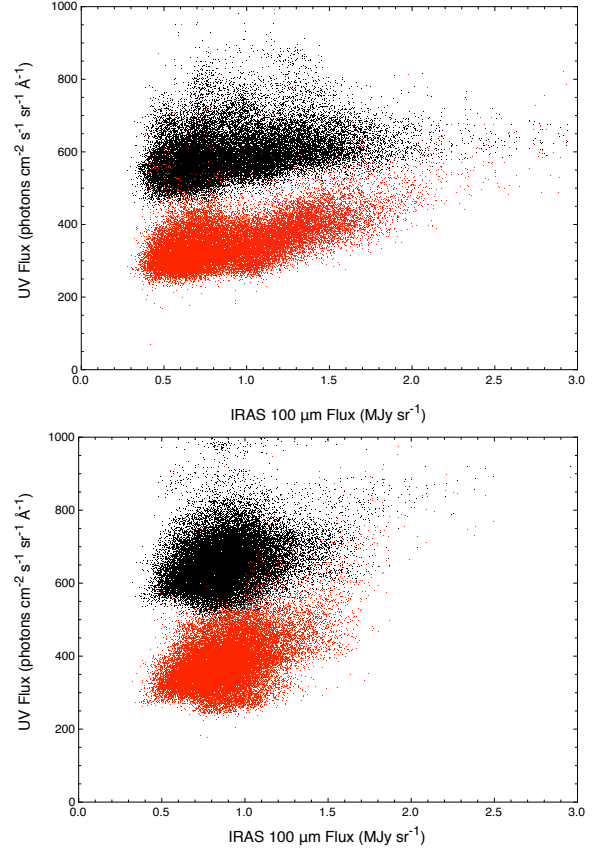
Figure 7. Distribution of FUV and NUV values in the NGP (black lines) and the SGP (red dashed lines). The area under each curve is scaled to 1.

Table 2. Correlations in the NGP

Bands	r^a	a^b	b^c	χ^2
NGP				
FUV – IRAS	0.569	101	259	6.68
NUV – IRAS	0.350	63	535	2.27
E(B - V) – IRAS	0.742	0.027	-0.004	-
FUV – E(B-V)	0.486	2367	302	7.55
NUV – E(B-V)	0.191	954	573	2.49
NUV – FUV	0.524	0.536	405	7.50
NGP ($100\ \mu\text{m} < 0.8\ \text{MJy sr}^{-1}$)				
FUV – IRAS	0.173	86	273	6.49
NUV – IRAS	0.168	95	512	2.09
E(B - V) – IRAS	0.289	0.014	0.005	-
FUV – E(B-V)	0.031	326	322	6.68
NUV – E(B-V)	0.083	988	557	2.13
NUV – FUV	0.542	0.615	370	6.07
NGP ($100\ \mu\text{m} > 0.8\ \text{MJy sr}^{-1}$)				
FUV – IRAS	0.610	135	214	6.50
NUV – IRAS	0.160	34	573	2.37
E(B - V) – IRAS	0.710	0.037	-0.017	1.12
FUV – E(B-V)	0.498	2131	316	7.78
NUV – E(B-V)	0.026	107	611	2.43
NUV – FUV	0.399	0.387	469	8.17

^aCorrelation coefficient.^bScale factor: UV in photon units; IR in MJy sr⁻¹
E(B - V) in mag.^cOffset (photon units).**Table 3.** Correlations in the SGP

Bands	p^a	a^b	b^c	χ^2
SGP				
FUV – IRAS	0.476	170	237	11.13
NUV – IRAS	0.280	92	578	2.82
E(B - V) – IRAS	0.548	0.017	0.00	-
FUV – E(B-V)	0.397	4610	316	12.13
NUV – E(B-V)	0.214	2287	624	2.92
NUV – FUV	0.643	0.593	430	7.18
SGP ($100\ \mu\text{m} < 0.8$)				
FUV – IRAS	0.139	99	293	8.81
NUV – IRAS	0.120	87	582	2.31
E(B - V) – IRAS	0.237	0.011	0.005	-
FUV – E(B-V)	0.087	1306	344	8.92
NUV – E(B-V)	0.071	1078	628	2.33
NUV – FUV	0.623	0.635	412	5.72
SGP ($100\ \mu\text{m} > 0.8$)				
FUV – IRAS	0.487	224	179	12.13
NUV – IRAS	0.226	94	575	3.13
E(B - V) – IRAS	0.495	0.02	-0.003	0.38
FUV – E(B-V)	0.400	4502	326	13.36
NUV – E(B-V)	0.184	1882	638	3.18
NUV – FUV	0.626	0.570	440	8.01

^aCorrelation coefficient.^bScale factor: UV in photon units; IR in MJy sr⁻¹
E(B - V) in mag.^cOffset (photon units).**Figure 8.** NGP (top) and SGP (bottom). The FUV (red) lies below the NUV (black) in both poles.

(CIB) which [Lagache et al. \(2000\)](#) found to be 0.78 ± 0.21 MJy sr⁻¹ at $100\ \mu\text{m}$. The CIB, which may include an un-subtracted zodiacal light component of $0.3\ \text{MJy sr}^{-1}$ ([Dole et al. 2006](#)), represents that part of the IR background which is not correlated with interstellar dust and is analogous to the UV offsets in Tables 2 and 3.

Our surveyed region in the NGP overlaps part of the *GALEX* Ultraviolet Virgo Cluster Survey (GUVICS: [Boissier et al. \(2015\)](#)) with an excellent agreement in the areas of overlap, despite independent approaches to deriving the diffuse data from the *GALEX* observations. They averaged the E(B - V) over bins defined by the FUV and derived a correlation between them of $E(B - V) = -0.003845 + 8.77 \times 10^{-5} \times FUV$ (where FUV is in photon units) and suggested that the FUV flux may be used to calculate the E(B - V) at a higher spatial resolution and precision than either the *IRAS* data ([Schlegel et al. 1998](#)) or the *Planck* data ([Planck Collaboration et al. 2016](#)). We find very poor correlations between the UV fluxes and the *Planck* reddening ([Planck Collaboration et al. 2016](#)) (Tables 2 and 3), perhaps reflecting the uncertainty in the derived reddening at these low levels. When we bin, as they did, over the FUV, we do obtain a clear increase in the E(B - V) with the FUV (Fig. 9) but no clear prescription for calculating one from the other. As [Boissier et al. \(2015\)](#) point out, the FUV emission is dependent on the geometry of the stars and the dust, and while linear relations may hold over small regions, care has to be taken over larger areas of the sky.

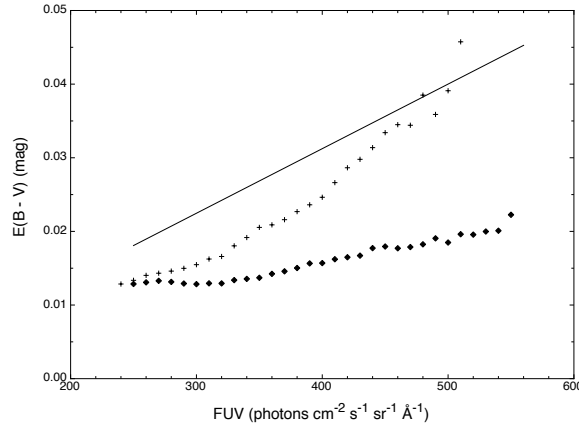


Figure 9. $E(B - V)$ from Planck Collaboration et al. (2016) plotted as a function of FUV for the NGP (plus signs) and the SGP (diamonds), where the reddening has been averaged over the FUV bins. The line shows the relation derived by Boissier et al. (2015).

Table 4. UV/IR Correlations

Region	λ^1	Slope ²	Offset ³
Hurwitz et al. (1991)	1620	300 ± 150	—
Perault et al. (1991)	1690	$214 - 244$	—
Wright (1992)	1500	203	—
Haikala et al. (1995)	1600	128 ± 3	-264 ± 9
Sasseen et al. (1995)	1600	233 ± 26	—
Sasseen & Deharveng (1996)	1600	33 ± 16	—
Schiminovich et al. (2001)	1740	58	$0 - 350$
Murthy et al. (2010)	1530	300	106
Murthy et al. (2010)	2310	220	193
Seon et al. (2011)	1540	158.3 ± 11.7	243.1 ± 44.4
Hamden et al. (2013)	1530	82 ± 67	338 ± 98

¹ Wavelength (Å)

² photon units (MJy sr⁻¹)⁻¹

³ photon units

The UV/IR ratio is about 100 photon units (MJy sr⁻¹)⁻¹ in the NGP and 200 photon units (MJy sr⁻¹)⁻¹ in the SGP (Tables 2 and 3). Typical values in the Galaxy are between 200 — 300 photon units (MJy sr⁻¹)⁻¹ (Table 4), albeit with considerable variation. The lowest values were found near the Galactic poles with Sasseen & Deharveng (1996) and Hamden et al. (2013) finding ratios of 33 ± 16 and 82 ± 67 photon units (MJy sr⁻¹)⁻¹, respectively, in the FUV. We will simply note these differences here and will defer a detailed study of the UV/IR ratio to a later work.

3 MODELLING MILKY WAY RADIATION

Most of the DGL at low Galactic latitudes is unequivocally due to the scattering of the light of hot stars from interstellar dust and we have applied the model developed by Murthy (2016) to predict the amount of Galactic dust-scattered radiation in the polar regions. This model uses a Monte Carlo process to track photons emitted from stars with location and spectral type from the Hipparcos catalog (Perryman et al. 1997) and stellar spectra from Castelli & Kurucz (2004). We used the 3-dimensional extinction map derived from PanSTARRS data by Green et al. (2015) which has an angular resolution of about 14' at the poles. The ad-

vantage of these data over the approach used in Murthy (2016), where the total dust column in any direction was matched to Schlegel et al. (1998), is that the extinction and its location are measured directly. Our modelled dust distribution is shown in (Fig. 10) for both poles and is superficially similar in each case to the IR maps shown in Fig. 1 and Fig. 2, respectively. The distribution of the extinction with distance (along a specific line of sight) is shown in Fig. 11 and is consistent with a scale height of 125 pc (Marshall et al. 2006) and a cavity of about 50 pc radius around the Sun (Welsh et al. 2010). The scattering function is that of Henyey & Greenstein (1941) with the albedo (a) and phase function asymmetry factor ($g = \langle \cos \theta \rangle$) as free parameters and the extinction law is from the “Milky Way” model of Draine (2003).

The dust at both poles has been extensively investigated through polarization measurements (Markkanen 1979; Berdyugin et al. 1995; Berdyugin & Teerikorpi 1997; Berdyugin et al. 2000, 2001; Berdyugin & Teerikorpi 2002, 2016; Berdyugin et al. 2004, 2011, 2014). The polarization in the NGP was divided into two regions: Area I and Area II (Markkanen 1979), approximately corresponding to with the 100 μ m flux and the polarization being larger in Area II. Markkanen’s Cloud is clearly visible in the 100 μ m map and in the FUV but not in the NUV (Fig. 1). The overall extinction in both poles is low with the minimum values close to zero (Fong et al. 1987; McFadzean et al. 1983) except for limited areas where clouds are seen in the IR maps with peak values of $E(B - V)$ from 0.02 – 0.04 (Berdyugin et al. 2011). Berdyugin et al. (2014) found that the polarization was correlated with the IR maps with the caveat that the polarization maps probed the dust to a distance of about 400 pc while the IR emission measured the dust along the entire line of sight. Berdyugin & Teerikorpi (2016) note that there may be some dusty structures extending to high positive latitudes within Area I, as suggested by the distribution of dark and molecular clouds, in addition to the diffuse dust.

We have run our model for a range of optical constants and compared the predicted flux averaged over the entire area of the poles with the observed data (Fig. 12). Although the dust is optically thin, the flux increase is not linear with the albedo because of the contribution from multiply scattered photons from other parts of the Galaxy (Murthy 2016).

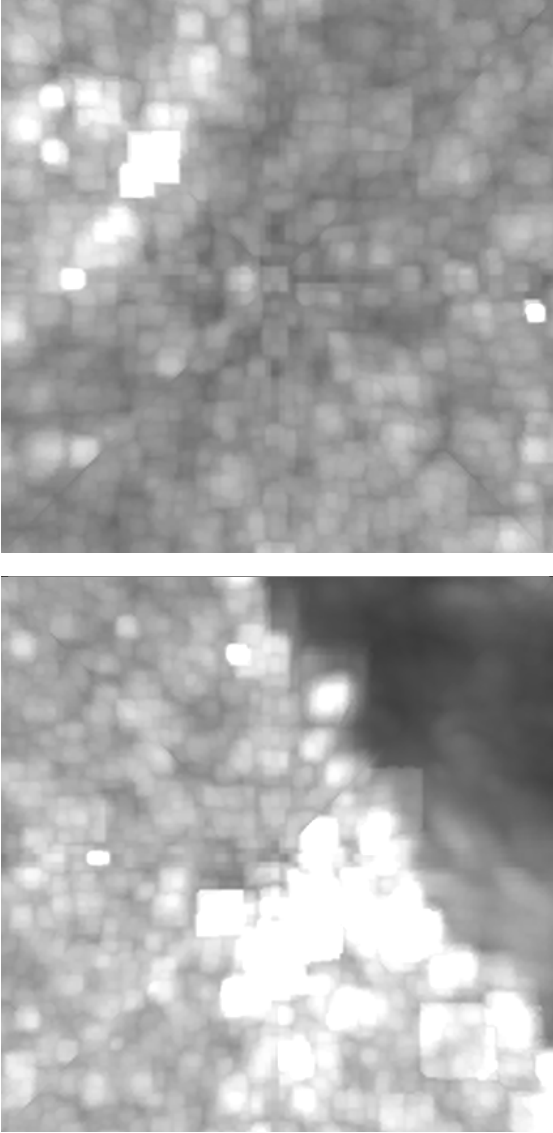


Figure 10. Modelled dust distribution ($E(B - V)$) at the NGP (top) and SGP (bottom). To be compared with the $100\ \mu\text{m}$ plots in Figs. 1 and 2.

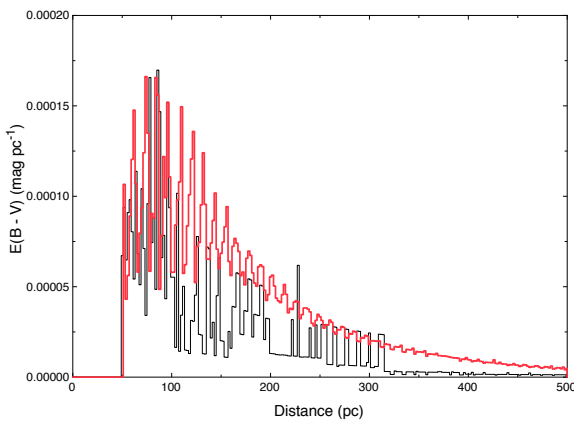


Figure 11. Modelled extinction as a function of distance for the NGP and SGP (red line).

Table 5. Components of the Diffuse Background

Component	Flux (photon units)
FUV NGP	
Observed	350
Dust	60
EGL	<150
Remainder	>140
FUV SGP	
Observed	390
Dust	90
EGL	<150
Remainder	>150
NUV NGP	
Observed	590
Dust	40
EGL	<150
Remainder	>400
NUV SGP	
Observed	660
Dust	60
EGL	<150
Remainder	>450

Most of the stellar photons come from the Galactic plane (Jura 1979); hence, the flux increases if the grains are scatter isotropically ($g = 0$) and many of the early papers suggested that the grains must scatter isotropically in order to explain the observed background.

Physical models of the interstellar grains suggest that $a \approx 0.4$ and $g \approx 0.5$ in the UV and we have tabulated the predictions of our model in Table 5. We find that the dust scattered component alone can account for about 20% of the total in the FUV and 10% in the NUV leaving about 150 photon units of “unexplained” radiation in the FUV and 400 photon units in the NUV.

This unknown source is unlikely to be associated with standard particle dark-matter candidates such as supersymmetric WIMPs or axions, at least in the most natural models (Henry et al. 2015). An alternative possibility is offered by primordial black holes (PBHs), which emit Hawking radiation with an approximately blackbody spectrum peaking at the characteristic energy $E = \hbar c^3 / (8\pi G M)$ where M is the characteristic PBH mass. Taking $E = 7$ eV (midway between our FUV and NUV energies), we obtain a putative PBH mass $M \approx 2 \times 10^{21}$ g, coinciding with one of the three remaining allowed PBH mass windows (Carr et al. 2016). This coincidence is intriguing enough that we briefly explore PBHs as a possible contributor to the unidentified component described above, whose bolometric intensity $Q_u = 4\pi I_\lambda \lambda \approx 7 \times 10^{-5}$ erg s $^{-1}$ cm $^{-2}$ with $I_\lambda \approx 250$ photons cm $^{-2}$ s $^{-1}$ sr $^{-1}$ Å $^{-1}$ at $\lambda \approx 2000$ Å.

PBH luminosity is exceedingly low, $L < \sim 2 \times 10^{-55} L_\odot (M/M_\odot)^{-2} \approx 6 \times 10^7$ erg s $^{-1}$ (Overduin and Wesson 2008). If these PBHs make up the cold dark matter in the halo of the Milky Way, then their local density $\rho \approx 0.008 M_\odot$ pc $^{-3}$ (Bovy & Tremaine 2012). If they are distributed uniformly, then the nearest one is

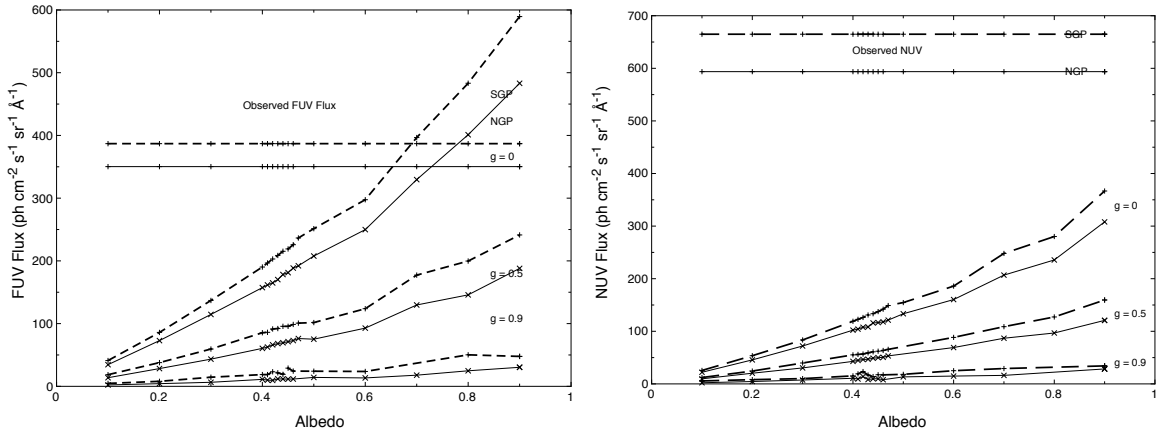


Figure 12. Modelled fluxes for the NGP (solid line) and the SGP (dashed line) fall short of the observed fluxes in both the FUV (left) and the NUV (right). We have integrated over the entire observed area in these plots.

located at a distance $\bar{r} = (\rho/M)^{-1/3} \approx 100$ AU. Its intensity $Q = L/(4\pi\bar{r}^2) \approx 2 \times 10^{-24}$ erg s $^{-1}$ cm $^{-2}$ as seen by us is far too low to account for Q_u . Alternatively, the total number of PBHs in the halo is $N = M_h/M \approx 1 \times 10^{24}$ where $M_h \approx 1 \times 10^{12} M_\odot$ (Xue et al. 2008). If these are clustered near the Galactic center at $R = 8$ kpc, its intensity $Q_h = NL/(4\pi R^2) \approx 2 \times 10^{-19}$ erg s $^{-1}$ cm $^{-2}$. This is still 15 orders of magnitude too small. More realistically, if the PBH halo extends beyond the Sun and can be regarded as approximately uniform in the solar vicinity, then $Q_h = \mathcal{L}R \approx 7 \times 10^{-17}$ erg s $^{-1}$ cm $^{-2}$ where luminosity density $\mathcal{L} = L\rho/M \approx 2 \times 10^{-33}$ erg s $^{-1}$ cm $^{-3}$. This still falls short of Q_u by 12 orders of magnitude, a discrepancy that cannot plausibly be attributed to non-uniformity in the PBH distribution. We infer that PBHs are not likely to contribute significantly to the astrophysical background, a conclusion reinforced by others (Frampton 2016). The failure of this explanation, of course, only deepens the mystery.

Our data are of much higher quality than our models, primarily because we do not know with precision the three-dimensional distribution of the dust, and our priority is to use the extinction maps and the infrared fluxes in conjunction with the *GALEX* data to develop a self-consistent model for the diffuse background in the polar regions. There is clearly a relation between the extinction as determined by Planck Collaboration et al. (2016) and the UV flux (Fig. 9) and the scatter in the UV fluxes must contain information about the small-scale clumping of the dust (Witt & Gordon 1996).

4 CONCLUSIONS

We have used *GALEX* data to study the diffuse ultraviolet background at both the North and South Galactic poles. The FUV data are correlated with the 100 μ m fluxes for IR fluxes greater than 0.8 MJy sr $^{-1}$, corresponding to the cosmic infrared background (CIB) of 0.78 MJy sr $^{-1}$ found by Lagache et al. (2000). There is no correlation of the NUV data with the IR, unlike at lower Galactic latitudes (Murthy 2014a).

The minimum flux in the FUV is 261 ± 34 photon units

and 249 ± 31 photon units in the NGP and SGP, respectively with the corresponding offsets in the NUV being 426 ± 15 (NGP) and 492 ± 35 (SGP) photon units. We have used a Monte Carlo model to predict the level of dust scattering and find that, with moderately forward-scattering grains ($a = 0.4$; $g = 0.5$), dust scattering can explain about 60 ± 20 photon units in either band with another 150 photon units from extragalactic sources. The remainder (150 photon units in the FUV and 400 photon units in the NUV) is due to an as yet unknown source.

We believe that the study of the Galactic poles will prove to be fruitful in differentiating between the Galactic and extragalactic (and terrestrial) components. Deep spectroscopy of the poles, including of cirrus features, would have been invaluable in separating the components but that seems unlikely in the near future with a dearth of UV missions expected. In its absence, we will continue our in-depth study of diffuse emission with *GALEX*.

ACKNOWLEDGEMENTS

We thank Prof. Berdyugin and Teerikorpi for clarifying the polarization results in the poles. Part of this research has been supported by the Department of Science and Technology under Grant IR/S2/PU-006/2012. This research has made use of NASA's Astrophysics Data System Bibliographic Services. We have used the GnuDataLanguage (<http://gnudatalanguage.sourceforge.net/index.php>) for the analysis of this data. The data presented in this paper were obtained from the Mikulski Archive for Space Telescopes (MAST). STScI is operated by the Association of Universities for Research in Astronomy, Inc., under NASA contract NAS5-26555. Support for MAST for non-HST data is provided by the NASA Office of Space Science via grant NNX09AF08G and by other grants and contracts.

REFERENCES

- Anderson R. C., Henry R. C., Brune W. H., Feldman P. D., Fastie W. G., 1979, *ApJ*, **234**, 415
- Berdyugin A., Teerikorpi P., 1997, *A&A*, **318**, 37

- Berdyugin A., Teerikorpi P., 2002, *A&A*, **384**, 1050
- Berdyugin A., Teerikorpi P., 2016, *A&A*, **587**, A79
- Berdyugin A., Snare M.-O., Teerikorpi P., 1995, *A&A*, **294**, 568
- Berdyugin A., Teerikorpi P., Haikala L., 2000, *A&A*, **358**, 717
- Berdyugin A., Teerikorpi P., Haikala L., Hanski M., Knude J., Markkanen T., 2001, *A&A*, **372**, 276
- Berdyugin A., Piirola V., Teerikorpi P., 2004, *A&A*, **424**, 873
- Berdyugin A., Piirola V., Teerikorpi P., 2011, in Bastien P., Manset N., Clemens D. P., St-Louis N., eds, *Astronomical Society of the Pacific Conference Series Vol. 449, Astronomical Polarimetry 2008: Science from Small to Large Telescopes*. p. 157
- Berdyugin A., Piirola V., Teerikorpi P., 2014, *A&A*, **561**, A24
- Boissier S., et al., 2015, *A&A*, **579**, A29
- Bovy J., Tremaine S., 2012, *ApJ*, **756**, 89
- Bowyer S., 1991, *ARA&A*, **29**, 59
- Carr B., Kühnel F., Sandstad M., 2016, *Phys. Rev. D*, **94**, 083504
- Castelli F., Kurucz R. L., 2004, *ArXiv Astrophysics e-prints*, Dole H., et al., 2006, *A&A*, **451**, A17
- Draine B. T., 2003, *A&A*, **41**, 241
- Driver S. P., et al., 2016, *ApJ*, **827**, 108
- Feldman P. D., Brune W. H., Henry R. C., 1981, *ApJ*, **249**, L51
- Fong R., Jones L. R., Shanks T., Stevenson P. R. F., Strong A. W., 1987, *MNRAS*, **224**, 1059
- Frampton P. H., 2016, *Modern Physics Letters A*, **31**, 1650093
- Gardner J. P., Brown T. M., Ferguson H. C., 2000, *ApJ*, **542**, L79
- Green G. M., et al., 2015, *ApJ*, **810**, 25
- Haikala L. K., Mattila K., Bowyer S., Sasseen T. P., Lampton M., Knude J., 1995, *ApJ*, **443**, L33
- Hamden E. T., Schiminovich D., Seibert M., 2013, *ApJ*, **779**, 180
- Henry R. C., 1991, *ARA&A*, **29**, 89
- Henry R. C., Murthy J., 1993, *ApJ*, **418**, L17
- Henry R. C., Murthy J., Overduin J., Tyler J., 2015, *ApJ*, **798**, 14
- Heney L. G., Greenstein J. L., 1941, *ApJ*, **93**, 70
- Hurwitz M., Bowyer S., Martin C., 1991, *ApJ*, **372**, 167
- Jakobsen P., Bowyer S., Kimble R., Jelinsky P., Grewing M., Kraemer G., Wulf-Mathies C., 1984, *A&A*, **139**, 481
- Joubert M., Deharveng J. M., Cruvellier P., Masnou J. L., Lequeux J., 1983, *A&A*, **128**, 114
- Jura M., 1979, *ApJ*, **227**, 798
- Kashikawa N., et al., 2004, *PASJ*, **56**, 1011
- Lagache G., Haffner L. M., Reynolds R. J., Tufte S. L., 2000, *A&A*, **354**, 247
- Ly C., et al., 2009, *ApJ*, **697**, 1410
- Madau P., 1992, *ApJ*, **389**, L1
- Markkanen T., 1979, *A&A*, **74**, 201
- Marshall D. J., Robin A. C., Reylé C., Schultheis M., Picaud S., 2006, *A&A*, **453**, 635
- Martin C., Hurwitz M., Bowyer S., 1991, *ApJ*, **379**, 549
- Martin D. C., et al., 2005, *ApJ*, **619**, L1
- Matsuoka Y., Ienaka N., Kawara K., Oyabu S., 2011, *ApJ*, **736**, 119
- McFadzean A. D., Hilditch R. W., Hill G., 1983, *MNRAS*, **205**, 525
- Morrissey P., et al., 2007, *ApJS*, **173**, 682
- Murthy J., 2014a, *ApJS*, **213**, 32
- Murthy J., 2014b, *Ap&SS*, **349**, 165
- Murthy J., 2016, *MNRAS*, **459**, 1710
- Murthy J., Henry R. C., 1995, *ApJ*, **448**, 848
- Murthy J., Henry R. C., Sujatha N. V., 2010, *ApJ*, **724**, 1389
- Onaka T., Kodaira K., 1991, *ApJ*, **379**, 532
- Paresce F., Bowyer S., Lampton M., Margon B., 1979, *ApJ*, **230**, 304
- Paresce F., McKee C. F., Bowyer S., 1980, *ApJ*, **240**, 387
- Perault M., Lequeux J., Hanus M., Joubert M., 1991, *A&A*, **246**, 243
- Perryman M. A. C., et al., 1997, *A&A*, **323**
- Planck Collaboration et al., 2016, *A&A*, **586**, A132
- Sasseen T. P., Deharveng J.-M., 1996, *ApJ*, **469**, 691
- Sasseen T. P., Lampton M., Bowyer S., Wu X., 1995, *ApJ*, **447**, 630
- Schiminovich D., Friedman P. G., Martin C., Morrissey P. F., 2001, *ApJ*, **563**, L161
- Schlegel D. J., Finkbeiner D. P., Davis M., 1998, *ApJ*, **500**, 525
- Seon K.-I., et al., 2011, *ApJS*, **196**, 15
- Tennysen P. D., Henry R. C., Feldman P. D., Hartig G. F., 1988, *ApJ*, **330**, 435
- Voyer E. N., Gardner J. P., Teplitz H. I., Siana B. D., de Mello D. F., 2011, *ApJ*, **736**, 80
- Welsh B. Y., Lallemand R., Vergely J.-L., Raimond S., 2010, *A&A*, **510**, A54
- Witt A. N., Gordon K. D., 1996, *ApJ*, **463**, 681
- Wright E. L., 1992, *ApJ*, **391**, 34
- Xu C. K., et al., 2005, *ApJ*, **619**, L11
- Xue X. X., et al., 2008, *ApJ*, **684**, 1143

This paper has been typeset from a \LaTeX file prepared by the author.